

Jointly optimal denoising, dereverberation, and source separation

Tomohiro Nakatani, *Senior Member, IEEE*, Christoph Boeddeker, *Student Member, IEEE*,
Keisuke Kinoshita, *Senior Member, IEEE*, Rintaro Ikeshita, *Member, IEEE*,
Marc Delcroix, *Senior Member, IEEE*, Reinhold Haeb-Umbach, *Fellow, IEEE*

Abstract—This paper proposes methods that can optimize a Convolutional BeamFormer (CBF) for performing denoising, dereverberation, and source separation (DN+DR+SS) at the same time. Conventionally, cascade configuration composed of a Weighted Prediction Error minimization (WPE) dereverberation filter followed by a Minimum Variance Distortionless Response (MVDR) beamformer has been used as the state-of-the-art frontend of far-field speech recognition, however, overall optimality of this approach is not guaranteed. In the blind signal processing area, an approach for jointly optimizing dereverberation and source separation (DR+SS) has been proposed, however, this approach requires huge computing cost, and has not been extended for application to DN+DR+SS. To overcome the above limitations, this paper develops new approaches for optimizing DN+DR+SS in a computationally much more efficient way. To this end, we introduce two different techniques for factorizing a CBF into WPE filters and beamformers, one based on extension of the conventional joint optimization approach proposed for DR+SS and the other based on a novel factorization technique, and derive methods optimizing them for DN+DR+SS based on the maximum likelihood estimation using a neural network-supported steering vector estimation. Experiments using noisy reverberant sound mixtures show that the proposed optimization approaches greatly improve the performance of the speech enhancement in comparison with the conventional cascade configuration in terms of the signal distortion measures and ASR performance. It is also shown that the proposed approaches can greatly reduce the computing cost with improved estimation accuracy in comparison with the conventional joint optimization approach.

Index Terms—Beamforming, dereverberation, source separation, microphone array, automatic speech recognition, maximum likelihood estimation

I. INTRODUCTION

When a speech signal is captured by distant microphones, e.g., in a conference room, it often contains reverberation, diffuse noise, and extraneous speakers' voices. These components are detrimental to the intelligibility of the captured speech and often cause serious degradation in many applications such as hands-free teleconferencing and Automatic Speech Recognition (ASR).

Microphone array speech enhancement has been extensively studied to minimize the aforementioned detrimental effects in the acquired signal. For performing denoising (DN), beamforming techniques have been investigated for decades [1], [2], [3], [4], and the Minimum Variance Distortionless Response (MVDR) beamformer and the Minimum Power Distortionless

Response (MPDR) beamformer, are now widely used as the state-of-the-art techniques. For source separation (SS), a number of blind signal processing techniques have been developed, including independent component analysis [5], independent vector analysis [6], and spatial clustering-based beamforming [7]. For dereverberation (DR), a Weighted Prediction Error minimization (WPE) based linear prediction technique [8], [9] and its variants [10] have been actively studied as an effective approach. With these techniques, for determining the coefficients of the filtering, it is crucial to accurately estimate statistics of the speech signals and the noise, such as their spatial covariances and time-varying variances. However, the estimation often becomes inaccurate when the signals mixed under reverberant and noisy conditions, which seriously degrades the performance of these techniques.

To enhance the robustness of the above techniques, recently, neural network-supported microphone array speech enhancement has been actively studied, and showed its effectiveness for denoising [11], dereverberation [12], and source separation [13], [14]. With this approach, estimation of the statistics of the signals and noise, such as Time-Frequency (TF) masks and time-varying variances, is conducted by neural networks [13], [15], [16], [17], while speech enhancement is performed by the microphone array signal processing. This combination is particularly effective because neural networks can very well capture spectral patterns of signals over wide TF ranges, and can reliably estimate such statistics of the signals, which was not well handled by the conventional signal processing. On the other hand, neural networks often introduce nonlinear distortions into the processed signal, which are harmful to perceived speech quality and ASR, while it can be well avoided by microphone array techniques. A number of articles have reported the usefulness of this combination, particularly for far-field ASR, e.g., at the REVERB challenge [18] and the CHiME-3/4/5 challenges [19], [20].

Despite the success of the neural network-supported microphone array speech enhancement, it is still not yet well investigated how to optimally combine individual microphone array techniques for performing denoising, dereverberation, and source separation (DN+DR+SS) at the same time in a computationally efficient way. For example, for denoising and dereverberation (DN+DR), cascade configuration of a WPE filter followed by a MVDR/MPDR beamformer has been widely used as the state-of-the-art frontend, e.g., at the far-field ASR challenges [18], [19], [20], [21]. However, the WPE filter and the beamformer are separately optimized, and the

T. Nakatani, K. Kinoshita, R. Ikeshita, and M. Delcroix are with NTT Corporation. C. Boeddeker and R. Haeb-Umbach are with Paderborn Univ.
Manuscript received January 1, 2020; revised XXXX XX, 2020.

overall optimality of this approach is not guaranteed. In order to perform DN+DR in an optimal way, several techniques have been proposed using a Kalman filter [22], [23], [24]. A technique, called Integrated Sidelobe Cancellation and Linear Prediction (ISCLP) [24], optimizes an integrated filter that can cancel noise and reverberation from the observed signal using a sidelobe cancellation framework. With this technique, however, a steering vector of the target signal needs to be estimated in advance directly from noisy reverberant speech, which is a challenging problem, and thus limits the overall estimation accuracy. In the blind signal processing area, on the other hand, a technique to jointly optimize a pair of a WPE filter followed by a beamformer has been proposed for dereverberation and source separation (DR+SS) under noiseless conditions [25], [26], [27]. One advantage of this approach is that we can access multichannel dereverberated signals obtained as the output of the WPE filter during the optimization, and utilize them to reliably estimate the beamformer. However, this approach requires 1) huge computing cost for the optimization, and 2) has not been extended for application to DN+DR+SS.

To overcome the above limitations, this paper develops algorithms that can jointly optimize WPE filter(s) and beamformer(s) to perform DN+DR+SS in a computationally much more efficient way. For this purpose, we use a Convolutional BeamFormer (CBF) as a general form of a linear filter that can be factorized into WPE filter(s) and beamformer(s), and present an objective for DN+DR+SS based on the maximum likelihood estimation, on an assumption that the steering vectors of the desired signals are given, or can be estimated reliably using the output of the WPE filters obtained during the optimization. Two effective optimization algorithms are, then, derived for DN+DR+SS based on two different factorization approaches. The first approach, referred to as a source-packed factorization approach, is an extension of the conventional joint optimization technique proposed for DR+SS [25], [26], [27]. In this paper, we first show that direct application of this approach to DN+DR+SS has serious problems in terms of the computational efficiency and the estimation accuracy, and then present its extension for solving these problems. The second approach, referred to as a source-wise factorization approach, is based on a novel factorization technique. It factorizes a CBF into a set of sub-filter pairs, each of which is composed of a WPE filter and a beamformer, and aimed at estimating each source independently. A neural network supported TF-mask estimation technique is also incorporated into both approaches¹ for making the estimation of the steering vectors robust. While both approaches work comparably well in terms of the estimation accuracy, the source-wise factorization has advantages in terms of computational efficiency. An additional benefit of the source-wise factorization is that it can be used, without loss of optimality, for extraction of a single target source from a sound mixture, which is now an important application area of speech enhancement [13], [29].

Experiments based on noisy reverberant sound mixtures

created using the REVERB Challenge dataset [18] show that the proposed optimization approaches substantially improve the performance of DN+DR+SS in comparison to the conventional cascade configuration in terms of ASR performance and reduction of signal distortion. It is also shown that the two proposed approaches can greatly reduce the computing cost with improved estimation accuracy in comparison with the conventional joint optimization approach.

Certain parts of this paper have already been presented in our recent conference papers. In [30], ML formulation for optimizing a CBF was derived for DN+DR. In [31], it was shown that a CBF for DN+DR can be factorized into a WPE filter and a weighted MPDR (wMPDR) beamformer, and jointly optimized without loss of optimality. Furthermore, [32] presented ways to reliably estimate TF masks for DN+DR+SS. This paper integrates these techniques to perform DN+DR+SS using the source-wise factorization approach.

In the remainder of this paper, the model of the observed signal and that of the CBF are defined in Section II. Then, Section III presents the proposed optimization methods. Section IV summarizes characteristics and advantages of the proposed methods. In Sections V and VI, experimental results and concluding remarks are described, respectively.

II. MODELS OF SIGNAL AND BEAMFORMER

This paper assumes that I source signals are captured by $M(\geq I)$ microphones in a noisy reverberant environment. The captured signal at each TF point in the short-time Fourier transform (STFT) domain is modeled by

$$\mathbf{x}_{t,f} = \sum_{i=1}^I \mathbf{x}_{t,f}^{(i)} + \mathbf{n}_{t,f}, \quad (1)$$

$$\mathbf{x}_{t,f}^{(i)} = \mathbf{d}_{t,f}^{(i)} + \mathbf{r}_{t,f}^{(i)}, \quad (2)$$

where t and f are time and frequency indices, respectively, $\mathbf{x}_{t,f} = [x_{1,t,f}, \dots, x_{M,t,f}]^\top \in \mathbb{C}^{M \times 1}$ is a column vector containing all microphone signals at a TF point. Here, $(\cdot)^\top$ denotes the non-conjugate transpose. $\mathbf{x}_{t,f}^{(i)} = [x_{1,t,f}^{(i)}, \dots, x_{M,t,f}^{(i)}]^\top$ is a (noiseless) reverberant signal corresponding to the i th source, and $\mathbf{n}_{t,f} = [n_{1,t,f}, \dots, n_{M,t,f}]^\top$ is the additive diffuse noise. $\mathbf{x}_{t,f}^{(i)}$ for each source in Eq. (1) is further decomposed into two parts in Eq. (2), one consisting of the direct signal and early reflections, referred to as a desired signal $\mathbf{d}_{t,f}^{(i)}$, and the other corresponding to the late reverberation $\mathbf{r}_{t,f}^{(i)}$. Hereafter, the frequency indices of the symbols are omitted for brevity, on the assumption that each frequency bin is processed independently in the same way.

In this paper, the goal of DN+DR+SS is to estimate $\mathbf{d}_t^{(i)}$ for each source i from \mathbf{x}_t in Eq. (1) by reducing $\mathbf{r}_t^{(i)}$ for the source i , $\mathbf{x}_t^{(i')}$ for all the other sources $i' \neq i$, and the diffuse noise \mathbf{n}_t . It is known that in noisy reverberant environments the early reflections enhance the intelligibility of speech for human perception [33] and improve the ASR performance by computer [34], and thus we include them in the desired signal. Hereafter, this paper uses $m = 1$ as the reference microphone, and describes a method for estimating the desired signal, $d_{1,t}^{(i)}$, at the microphone without loss of generality.

¹It is worth noting that the proposed techniques can also be applied to the conventional blind signal processing for DR+SS as discussed in [28].

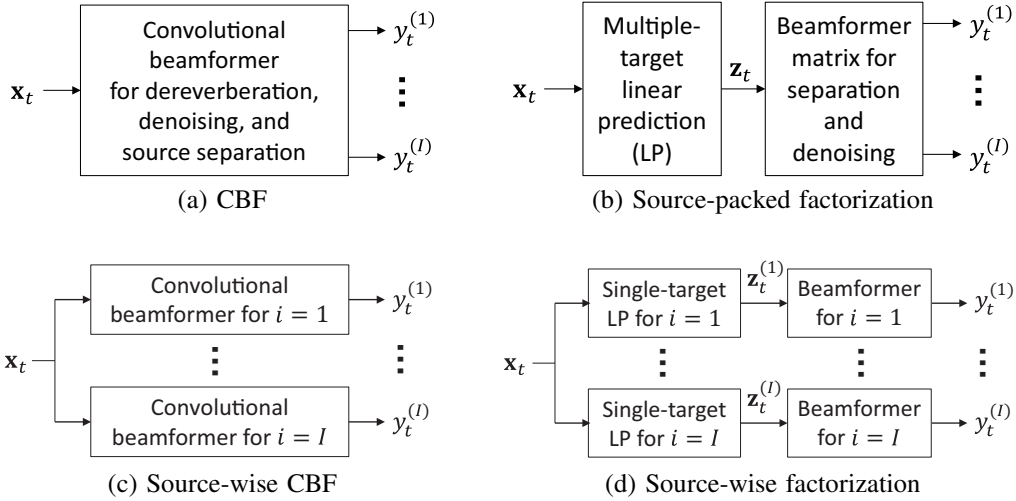


Fig. 1. A CBF and its three different implementations. They are equivalent to each other in the sense that whatever values are set to coefficients of one implementation, certain coefficients of the other implementations can be determined such that they realize the same input-output relationship. Thus, the optimal solutions of all the implementations are identical as long as they are optimized based on the same objective.

To achieve the above goal, we further model $\mathbf{d}_t^{(i)}$ as

$$\mathbf{d}_t^{(i)} = \mathbf{v}^{(i)} s_t^{(i)} = \tilde{\mathbf{v}}^{(i)} d_{1,t}^{(i)}, \quad (3)$$

where $s_t^{(i)}$ is the i th clean speech at a TF point. In Eq. (3), the desired signal of the i th source, $\mathbf{d}_t^{(i)}$, is modeled by $\mathbf{v}^{(i)} s_t^{(i)}$, i.e., a product in the STFT domain of the clean speech with a transfer function $\mathbf{v}^{(i)}$, hereafter referred to as a steering vector, assuming that the duration of the impulse response corresponding to the direct signal and early reflections in the time domain is sufficiently short in comparison with the analysis window [35]. Then, the desired signal is further rewritten as $\tilde{\mathbf{v}}^{(i)} d_{1,t}^{(i)}$, i.e., a product of the desired signal at the reference microphone $d_{1,t}^{(i)} = v_1^{(i)} s_t^{(i)}$ with a Relative Transfer Function (RTF) [36] which is defined as the steering vector divided by its reference microphone element, namely

$$\tilde{\mathbf{v}}^{(i)} = \mathbf{v}^{(i)} / v_1^{(i)}. \quad (4)$$

In contrast, assuming that the duration of the late reverberation in the time domain is larger than the analysis window, the late reverberation $\mathbf{r}_t^{(i)}$ is modeled by a convolution in the STFT domain [37] of the clean speech with a time series of acoustic transfer functions corresponding to the late reverberation as

$$\mathbf{r}_t^{(i)} = \sum_{\tau=\Delta}^{L_a-1} \mathbf{a}_\tau^{(i)} s_{t-\tau}^{(i)}, \quad (5)$$

where $\mathbf{a}_\tau^{(i)} = [a_{1,\tau}^{(i)}, \dots, a_{M,\tau}^{(i)}]^\top$ for $\tau \in \{\Delta, \dots, L_a - 1\}$ are the acoustic transfer functions, and Δ is the relative frame delay of the late reverberation start time to the direct signal.

In this paper, we assume that $\mathbf{d}_t^{(i)}$ is statistically independent² of $s_{t'}^{(i)}$ for $t - t' \geq \Delta$, and thus statistically independent of $\mathbf{x}_{t'}^{(i)}$ for $t - t' \geq \Delta$ and $\mathbf{r}_{t'}^{(i)}$ for $t - t' \geq 0$. In addition, we assume $\mathbf{d}_t^{(i)}$ is statistically independent of $\mathbf{x}_{t'}^{(i')}$ and $\mathbf{n}_{t'}$ for all t, t' and $i' \neq i$.

²See [8] for more precise discussion on the statistical independence between $\mathbf{d}_t^{(i)}$ and s_t .

A. Definition of a CBF and its three different implementations

We define a CBF shown in Fig. 1 (a), which will later be factorized into WPE filter(s) and beamformer(s), as

$$\mathbf{y}_t = \mathbf{W}_0^H \mathbf{x}_t + \sum_{\tau=\Delta}^{L-1} \mathbf{W}_\tau^H \mathbf{x}_{t-\tau}, \quad (6)$$

where $\mathbf{y}_t = [y_t^{(1)}, \dots, y_t^{(I)}]^\top \in \mathbb{C}^{I \times 1}$ is the output of the CBF corresponding to estimates of I desired signals, $\mathbf{W}_\tau \in \mathbb{C}^{M \times I}$ for each $\tau \in \{0, \Delta, \Delta+1, \dots, L-1\}$ is a matrix composed of the beamformer coefficients, $(\cdot)^H$ denotes conjugate transpose, and Δ is the prediction delay that corresponds to Δ in Eq. (3). In Eqs. (6), due to the use of Δ , the desired signals included in the first term can be statistically independent of the second term according to the assumptions introduced in the signal model. This paper performs DN+DR+SS by estimating appropriate beamformer coefficients based on Eqs. (6).

In the following, we present three different implementations of the CBF (Figs. 1 (b)-(d)).

1) *Source-packed factorization*: With the simultaneous factorization shown in Fig. 1 (b), we directly factorize³ the CBF in Eq. (6) as $\mathbf{W}_0 = \mathbf{Q}$ and $\overline{\mathbf{W}} = -\overline{\mathbf{G}}\mathbf{Q}$ where $\mathbf{Q} \in \mathbb{C}^{M \times I}$, $\overline{\mathbf{G}} \in \mathbb{C}^{M(L-\Delta) \times M}$, and

$$\overline{\mathbf{W}} = [\mathbf{W}_\Delta^\top, \dots, \mathbf{W}_{L-1}^\top]^\top \in \mathbb{C}^{M(L-\Delta) \times I}. \quad (7)$$

Then, Eq. (6) can be rewritten as a pair of a (convolutional) linear prediction filter followed by a (non-convolutional) beamformer matrix, respectively, defined as

$$\mathbf{z}_t = \mathbf{x}_t - \overline{\mathbf{G}}^H \overline{\mathbf{x}}_t, \quad (8)$$

$$\mathbf{y}_t = \mathbf{Q}^H \mathbf{z}_t. \quad (9)$$

Here, $\overline{\mathbf{x}}_t$ is a column vector containing a time series of past multichannel observed signal defined as

$$\overline{\mathbf{x}}_t = [\mathbf{x}_{t-\Delta}^\top, \dots, \mathbf{x}_{t-L+1}^\top]^\top \in \mathbb{C}^{M(L-\Delta) \times 1}, \quad (10)$$

³The existence of $\overline{\mathbf{G}}$ that satisfies $\overline{\mathbf{W}} = -\overline{\mathbf{G}}\mathbf{Q}$ is guaranteed for any $\overline{\mathbf{W}}$ when $M \geq I$ and $\text{rank}\{\mathbf{Q}\} = I$.

$\mathbf{z}_t \in \mathbb{C}^{M \times 1}$ and $\overline{\mathbf{G}}$ are the output and the prediction matrix of the linear prediction, and \mathbf{Q} is the coefficient matrix of the beamformer. Eq. (8) is supposed to dereverberate all the sources at the same time, and thus referred to as a multiple-target linear prediction, while Eq. (9) is supposed to perform denoising and source separation at the same time. Because the factorization is applied simultaneously for all the sources, this is called source-packed factorization.

Based on the source-packed factorization, cascade configuration composed of a WPE filter followed by a beamformer has been widely used for DN+DR+SS in the far-field speech recognition area [14], [20], [38], and joint optimization of a WPE filter and a beamformer has been investigated for DR+SS in the blind signal processing area [25], [26], [27].

2) *Source-wise CBF*: Next, we define a source-wise CBF shown in Fig. 1 (c). It is obtained by decomposing \mathbf{W}_τ for each τ as

$$\mathbf{W}_\tau = [\mathbf{w}_\tau^{(1)}, \dots, \mathbf{w}_\tau^{(I)}], \quad (11)$$

where $\mathbf{w}_\tau^{(i)} = [w_{1,\tau}^{(i)}, w_{2,\tau}^{(i)}, \dots, w_{M,\tau}^{(i)}]^\top \in \mathbb{C}^{M \times 1}$ is a column vector that is used to extract the i th desired signal. Then, Eq. (6) can be rewritten for each source i as

$$y_t^{(i)} = \left(\mathbf{w}_0^{(i)}\right)^H \mathbf{x}_t + \sum_{\tau=\Delta}^{L-1} \left(\mathbf{w}_\tau^{(i)}\right)^H \mathbf{x}_{t-\tau}. \quad (12)$$

3) *Source-wise factorization*: With the source-wise factorization shown in Fig. 1 (d), we further factorize Eq. (12) for each source i as $\mathbf{w}_0^{(i)} = \mathbf{q}^{(i)}$ and $\overline{\mathbf{w}}^{(i)} = -\overline{\mathbf{G}}^{(i)} \mathbf{q}^{(i)}$ where $\mathbf{q}^{(i)} \in \mathbb{C}^{M \times 1}$, $\overline{\mathbf{G}}^{(i)} \in \mathbb{C}^{M(L-\Delta) \times M}$, and

$$\overline{\mathbf{w}}^{(i)} = \left[\left(\mathbf{w}_\Delta^{(i)}\right)^\top, \dots, \left(\mathbf{w}_{L-1}^{(i)}\right)^\top \right]^\top \in \mathbb{C}^{M(L-\Delta) \times 1}. \quad (13)$$

Then, Eq. (12) can be rewritten as a pair of a linear prediction filter followed by a beamformer, respectively, defined as

$$\mathbf{z}_t^{(i)} = \mathbf{x}_t - \left(\overline{\mathbf{G}}^{(i)}\right)^H \overline{\mathbf{x}}_t, \quad (14)$$

$$y_t^{(i)} = \left(\mathbf{q}^{(i)}\right)^H \mathbf{z}_t^{(i)}, \quad (15)$$

where $\mathbf{z}_t^{(i)} \in \mathbb{C}^{M \times 1}$ and $\overline{\mathbf{G}}^{(i)}$ are the output and the prediction matrix of the linear prediction, and $\mathbf{q}^{(i)}$ is the coefficient vector of the beamformer. Because Eq. (14) is performed only for estimation of the i th source, it is referred to as a single-target linear prediction.

4) *Relationship between two factorization approaches*: The difference between the two factorization approaches, namely Fig. 1 (b) and (d), is based only on the way to perform linear prediction, Eq. (8) or Eq. (14), and more specifically based on whether the prediction matrices, $\overline{\mathbf{G}}$ and $\overline{\mathbf{G}}^{(i)}$, are common to all the sources or different over different sources. According to this, different optimization algorithms with different characteristics are derived, as will be shown in Section III. In contrast, the beamformer parts, \mathbf{Q} and $\mathbf{q}^{(i)}$ in Eqs. (12) and (15) are identical to each other between the two approaches, viewing $\mathbf{q}^{(i)}$ as the i th column of \mathbf{Q} .

It should be noted that all the above implementations of a CBF are equivalent to each other in the sense that whatever

values are set to coefficients of one implementation, certain coefficients of the other implementations can be determined such that they realize the same input-output relationship. Thus, the optimal solutions of all the implementations are identical as long as they are based on the same objective.

III. ML ESTIMATION OF CBF

In this section, two different optimization algorithms are derived, respectively, using (b) source-packed and (d) source-wise factorization. For the derivation, we assume that the RTFs $\tilde{\mathbf{v}}^{(i)}$ and the time-varying variances $\lambda_t^{(i)}$ are given, and later in Section III-E describe a way for estimating $\lambda_t^{(i)}$ jointly with the CBF coefficients based on the ML criterion, and that for estimating $\tilde{\mathbf{v}}^{(i)}$ based on the output of the WPE filter obtained at a step of the optimization.

A. Probabilistic model

First, we formulate the objective for DN+DR+SS by reinterpreting the objective for DN+DR presented in [30]. That is, we interpret DN+DR+SS as a processing that separately enhances each source i by reducing the late reverberation of the source (DR) and by reducing the other sources and the diffuse noise as the additive noise (DN). With this interpretation, we introduce the following assumptions similar to [30].

- The output of the optimal CBF for each i , namely $y_t^{(i)}$, follows zero-mean complex Gaussian distribution with a time-varying variance $\lambda_t^{(i)} = \mathbb{E} \left\{ \left| y_t^{(i)} \right|^2 \right\}$ [8].
- The beamformer satisfies a distortionless constraint for each source i defined using the RTF $\tilde{\mathbf{v}}^{(i)}$ in Eq. (4) as

$$\left(\mathbf{w}_0^{(i)}\right)^H \tilde{\mathbf{v}}^{(i)} = 1 \quad \left(\text{or} \quad \left(\mathbf{q}^{(i)}\right)^H \tilde{\mathbf{v}}^{(i)} = 1\right). \quad (16)$$

Then, according to the discussion in [30], we can approximately derive the objective to minimize for estimating the CBF coefficients for source i , e.g., $\theta^{(i)} = \{\mathbf{w}_0^{(i)}, \overline{\mathbf{w}}^{(i)}\}$, based on the ML estimation as

$$\mathcal{L}_i(\theta^{(i)}) = \frac{1}{T} \sum_{t=1}^T \left(\frac{\left| y_t^{(i)} \right|^2}{\lambda_t^{(i)}} + \log \lambda_t^{(i)} \right) \quad \text{s.t.} \quad \left(\mathbf{w}_0^{(i)}\right)^H \tilde{\mathbf{v}}^{(i)} = 1. \quad (17)$$

The objective for estimating all the sources can then be obtained by summing Eq. (17) over all the sources as

$$\mathcal{L}(\Theta) = \sum_{i=1}^I \mathcal{L}_i(\theta^{(i)}), \quad \text{s.t.} \quad \left(\mathbf{w}_0^{(i)}\right)^H \tilde{\mathbf{v}}^{(i)} = 1 \quad \text{for all } i, \quad (18)$$

where $\Theta = \{\theta^{(1)}, \dots, \theta^{(I)}\}$. This objective is used commonly for all the implementations of a CBF. In this paper, we call a CBF optimized by the above objective as weighted MPDR (wMPDR) CBF because it minimizes the average power of the output $y_t^{(i)}$ weighted by the time-varying variance.

Here, let us briefly explain how DN+DR+SS is performed by Eqs. (17) and (18). Substituting Eqs. (1) and (2) in Eq. (12) and using the distortionless constraint, we obtain

$$y_t^{(i)} = d_{1,t}^{(i)} + \hat{r}_t^{(i)} + \sum_{i' \neq i} \hat{x}_t^{(i')} + \hat{n}_t, \quad (19)$$

where $\hat{r}_t^{(i)}$, $\hat{x}_t^{(i')}$ for $i' \neq i$, and \hat{n}_t are late reverberation of the i th source, all the other sources, and the additive diffuse noise remaining in the output of the CBF, respectively, written using the source-wise CBF form as

$$\hat{r}_t^{(i)} = \left(\mathbf{w}_0^{(i)}\right)^H \mathbf{r}_t^{(i)} + \sum_{\tau=\Delta}^{L-1} \left(\mathbf{w}_\tau^{(i)}\right)^H \mathbf{x}_{t-\tau}^{(i)}, \quad (20)$$

$$\hat{x}_t^{(i')} = \left(\mathbf{w}_0^{(i)}\right)^H \mathbf{x}_t^{(i')} + \sum_{\tau=\Delta}^{L-1} \left(\mathbf{w}_\tau^{(i)}\right)^H \mathbf{x}_{t-\tau}^{(i')}, \quad (21)$$

$$\hat{n}_t = \left(\mathbf{w}_0^{(i)}\right)^H \mathbf{n}_t + \sum_{\tau=\Delta}^{L-1} \left(\mathbf{w}_\tau^{(i)}\right)^H \mathbf{n}_{t-\tau}, \quad (22)$$

According to the statistical independence assumptions introduced in Section II, $d_{1,t}^{(i)}$ is statistically independent of $\hat{r}_t^{(i)}$, $\hat{x}_t^{(i')}$, and \hat{n}_t . Then, substituting Eq. (19) in Eq. (17) and omitting constant terms, we obtain in the expectation sense

$$\mathbb{E} \left\{ \mathcal{L}_i(\theta^{(i)}) \right\} = \frac{1}{T} \sum_{t=1}^T \frac{\mathbb{E} \left\{ \left| \hat{r}_t^{(i)} + \sum_{i' \neq i} \hat{x}_t^{(i')} + \hat{n}_t \right|^2 \right\}}{\lambda_t^{(i)}}. \quad (23)$$

The above equation indicates that minimization of the objective minimizes sum of $\hat{r}_t^{(i)}$, $\hat{x}_t^{(i')}$ for $i' \neq i$, and \hat{n}_t in Eq. (19).

Before deriving the optimization algorithms, we define a matrix that is frequently used in the derivation, referred to as a variance-normalized spatio-temporal covariance matrix. Letting $\underline{\mathbf{x}}_t$ be a column vector composed of the current and past observed signals at all the microphones, defined as

$$\underline{\mathbf{x}}_t = [\mathbf{x}_t^\top, \bar{\mathbf{x}}_t^\top]^\top \in \mathbb{C}^{M(L-\Delta+1) \times 1}, \quad (24)$$

the matrix is defined as

$$\underline{\mathbf{R}}_{\mathbf{x}}^{(i)} = \frac{1}{T} \sum_{t=1}^T \frac{\underline{\mathbf{x}}_t \underline{\mathbf{x}}_t^H}{\lambda_t^{(i)}} \in \mathbb{C}^{M(L-\Delta+1) \times M(L-\Delta+1)}. \quad (25)$$

A factorized form of the matrix is also defined as

$$\underline{\mathbf{R}}_{\mathbf{x}}^{(i)} = \begin{bmatrix} \mathbf{R}_{\mathbf{x}}^{(i)} & \left(\mathbf{P}_{\mathbf{x}}^{(i)}\right)^H \\ \mathbf{P}_{\mathbf{x}}^{(i)} & \bar{\mathbf{R}}_{\mathbf{x}}^{(i)} \end{bmatrix}, \quad (26)$$

where

$$\mathbf{R}_{\mathbf{x}}^{(i)} = \frac{1}{T} \sum_{t=1}^T \frac{\mathbf{x}_t \mathbf{x}_t^H}{\lambda_t^{(i)}} \in \mathbb{C}^{M \times M}, \quad (27)$$

$$\mathbf{P}_{\mathbf{x}}^{(i)} = \frac{1}{T} \sum_{t=1}^T \frac{\bar{\mathbf{x}}_t \mathbf{x}_t^H}{\lambda_t^{(i)}} \in \mathbb{C}^{M(L-\Delta) \times M}, \quad (28)$$

$$\bar{\mathbf{R}}_{\mathbf{x}}^{(i)} = \frac{1}{T} \sum_{t=1}^T \frac{\bar{\mathbf{x}}_t \bar{\mathbf{x}}_t^H}{\lambda_t^{(i)}} \in \mathbb{C}^{M(L-\Delta) \times M(L-\Delta)}. \quad (29)$$

B. Optimization based on source-packed factorization

This subsection discusses methods for optimizing a CBF with the source-packed factorization. After describing a method for directly applying the conventional joint optimization technique used for DR+SS to DN+DR+SS, we summarize the problems in it, and present the solutions to the problems.

1) *Direct application of conventional technique:* With the source-packed factorization in Eqs. (8) and (9), it is difficult to estimate both \mathbf{Q} and $\bar{\mathbf{G}}$ at the same time in a closed form way even when $\lambda_t^{(i)}$ and $\tilde{\mathbf{v}}^{(i)}$ are all given. Instead, we use an iterative and alternate estimation scheme, following the idea from the blind signal processing technique [25], [26], [27], where at each estimation step, one of \mathbf{Q} and $\bar{\mathbf{G}}$ is updated while fixing the other.

For updating $\bar{\mathbf{G}}$, we fix \mathbf{Q} at its previously estimated value. For the derivation, the representation of linear prediction in Eq. (8) is slightly modified as

$$\mathbf{z}_t = \mathbf{x}_t - \bar{\mathbf{X}}_t \bar{\mathbf{g}}, \quad (30)$$

where $\bar{\mathbf{X}}_t$ and $\bar{\mathbf{g}}$ are equivalent to $\bar{\mathbf{x}}_t$ and $\bar{\mathbf{G}}$ with modified matrix structure defined as

$$\bar{\mathbf{X}}_t = \mathbf{I}_M \otimes \bar{\mathbf{x}}_t^\top \in \mathbb{C}^{M \times M^2(L-\Delta)}, \quad (31)$$

$$\bar{\mathbf{g}} = [\bar{\mathbf{g}}_1^\top, \dots, \bar{\mathbf{g}}_M^\top]^\top \in \mathbb{C}^{M^2(L-\Delta) \times 1}, \quad (32)$$

where $\mathbf{I}_M \in \mathbb{R}^{M \times M}$ is the identity matrix, \otimes is Kronecker product, and $\bar{\mathbf{g}}_m$ is the m th column of $\bar{\mathbf{G}}$. Then, considering that the CBF in Eqs. (8) and (9) can be written as $y_t^{(i)} = (\mathbf{q}^{(i)})^H (\mathbf{x}_t - \bar{\mathbf{X}}_t \bar{\mathbf{g}})$ and omitting normalization terms, the objective in Eq. (18) becomes

$$\mathcal{L}_{\bar{\mathbf{g}}}(\bar{\mathbf{g}}) = \frac{1}{T} \sum_{t=1}^T \|\mathbf{x}_t - \bar{\mathbf{X}}_t \bar{\mathbf{g}}\|_{\Phi_{\mathbf{q},t}}^2, \quad (33)$$

where $\|\mathbf{x}\|_{\mathbf{R}}^2 = \mathbf{x}^H \mathbf{R} \mathbf{x}$, and $\Phi_{\mathbf{q},t}$ is a semi-definite Hermitian matrix defined as

$$\Phi_{\mathbf{q},t} = \sum_{i=1}^I \frac{\mathbf{q}^{(i)} (\mathbf{q}^{(i)})^H}{\lambda_t^{(i)}} \in \mathbb{C}^{M \times M}. \quad (34)$$

Because Eq. (33) is a quadratic form with a lower bound, $\bar{\mathbf{g}}$ that minimizes it can be obtained as

$$\bar{\mathbf{g}} = \Psi^+ \boldsymbol{\psi}, \quad (35)$$

$$\Psi = \frac{1}{T} \sum_t \bar{\mathbf{X}}_t^H \Phi_{\mathbf{q},t} \bar{\mathbf{X}}_t \in \mathbb{C}^{M^2(L-\Delta) \times M^2(L-\Delta)}, \quad (36)$$

$$\boldsymbol{\psi} = \frac{1}{T} \sum_t \bar{\mathbf{X}}_t^H \Phi_{\mathbf{q},t} \mathbf{x}_t \in \mathbb{C}^{M^2(L-\Delta) \times 1}, \quad (37)$$

where $(\cdot)^+$ is the Moore-Penrose pseudo-inverse. Because the rank of Ψ is equal to or smaller than $MI(L-\Delta)$ as will be shown in Section III-B2, Ψ is rank deficient for over-determined cases, namely when $M > I$, and thus the use of the pseudo-inverse is indispensable. Eqs. (35) to (37) are equivalent to those used in the dereverberation step for the blind signal processing technique [25], [26], [27] except that in this paper denoising is additionally included in the objective and that over-determined cases are also considered. This filter is referred to as the multiple-target WPE filter in this paper.

For the update of \mathbf{Q} , fixing $\bar{\mathbf{g}}$ at its previously estimated value, the objective in Eq. (18) can be rewritten as

$$\mathcal{L}_{\mathbf{Q}}(\mathbf{Q}) = \sum_{i=1}^I \left\| \mathbf{q}^{(i)} \right\|_{\mathbf{R}_z^{(i)}}^2 \quad \text{s.t.} \quad (\mathbf{q}^{(i)})^H \tilde{\mathbf{v}}^{(i)} = 1, \quad (38)$$

where $\mathbf{R}_z^{(i)}$ is a variance-normalized spatial covariance matrix of the output of the multiple-target WPE filter, calculated as

$$\mathbf{R}_z^{(i)} = \frac{1}{T} \sum_{t=1}^T \frac{\mathbf{z}_t \mathbf{z}_t^H}{\lambda_t^{(i)}}. \quad (39)$$

Then, $\mathbf{q}^{(i)}$ that minimizes Eq. (38) under the distortionless constraint $(\mathbf{q}^{(i)})^H \tilde{\mathbf{v}}^{(i)} = 1$ can be obtained as

$$\mathbf{q}^{(i)} = \frac{(\mathbf{R}_z^{(i)})^{-1} \tilde{\mathbf{v}}^{(i)}}{(\tilde{\mathbf{v}}^{(i)})^H (\mathbf{R}_z^{(i)})^{-1} \tilde{\mathbf{v}}^{(i)}}. \quad (40)$$

Because the above beamformer minimizes the average power of \mathbf{z}_t weighted by the time-varying variance, we call this as weighted MPDR (wMPDR) beamformer^{4,5}.

The above algorithm, however, has two serious problems. Firstly, the size of the covariance matrix in Eq. (36) is very large, requiring huge computing cost for calculating it and its inverse. Secondly, as will be shown in the experiments, the iterative and alternate estimation of \mathbf{Q} and $\overline{\mathbf{G}}$ tends to converge to a sub-optimal point. This is probably because the objective defined by Eq. (18) is not suitable for over-determined cases with the source-packed factorization approach. That is, the objective evaluates only the output of the beamformer \mathbf{Q} while components that are relevant for the estimation of $\overline{\mathbf{G}}$ may be reduced in the beamformer output. This can happen with over-determined cases because the signal subspace dimension is reduced by the beamformer.

2) *Proposed extension:* Here, we present two techniques to mitigate the above problems within the source-packed factorization approach. The first one is used to reduce the computing cost. As shown in Appendix A, Eqs. (36) and (37) can be rewritten, using Eq. (26), as

$$\Psi = \sum_{i=1}^I \left(\mathbf{q}^{(i)} (\mathbf{q}^{(i)})^H \otimes (\overline{\mathbf{R}}_x^{(i)})^T \right), \quad (41)$$

$$\psi = \sum_{i=1}^I \left(\mathbf{q}^{(i)} \otimes (\mathbf{P}_x^{(i)} \mathbf{q}^{(i)})^* \right), \quad (42)$$

where $()^*$ denotes complex conjugate. In the above equations, the majority of the calculation is coming from that of $\overline{\mathbf{R}}_x^{(i)}$. Because the size of the matrix is much smaller than that of Ψ , we can greatly reduce the computing cost with this modification in comparison with direct calculation of Eqs. (36) and (37). Although we still need to calculate the inverse of the huge matrix Ψ even with this modification, the cost is relatively small in comparison with the direct calculation of Ψ . (Note that the rank of Ψ can be shown, based on Eq. (41), to be equal to or smaller than $MI(L - \Delta)$.)

⁴A wMPDR beamformer is a special case of a source-wise CBF, which was first proposed in [39] and will be presented by Eq. (49) in this paper. A source-wise CBF is reduced to a wMPDR beamformer when setting the length of the CBF $L = 1$, i.e., by just making it a non-convolutional beamformer.

⁵A wMPDR beamformer is also called a Maximum-Likelihood Distortionless Response (MLDR) beamformer in [40], but we do not use this name because other beamformers, including the MVDR beamformer, can also be derived based on the maximum-likelihood estimation.

The second technique introduces a heuristic to improve the update of the WPE filter. We modify the CBF to output not only I desired signals, but also $M - I$ auxiliary signals included in the orthogonal complement \mathbf{Q}^\perp of \mathbf{Q} , and model the auxiliary signals as zero-mean time-varying complex Gaussians. With this modification, the optimization is performed by calculating the summation in Eqs. (41) and (42) over not only $1 \leq i \leq I$ but also $I < i \leq M$, letting $\mathbf{q}^{(I+1)}, \dots, \mathbf{q}^{(M)}$ be the orthonormal bases for the orthogonal complement \mathbf{Q}^\perp . Because it is not important to distinguish the variances $\lambda_t^{(i)}$ of the auxiliary signals, we use the same value for them calculated as

$$\lambda_t^\perp = \left| \left(\sum_{i=I+1}^M \mathbf{q}^{(i)} \right)^H \mathbf{z}_t \right|^2, \quad (43)$$

and calculate \mathbf{P}_x^\perp and $\overline{\mathbf{R}}_x^\perp$ based on Eqs. (28) and (29) accordingly. In summary, we can implement this modification by adding the following terms, respectively, to Ψ and ψ in Eqs. (41) and (42).

$$\Psi^\perp = \left(\sum_{i=I+1}^M \mathbf{q}^{(i)} (\mathbf{q}^{(i)})^H \right) \otimes (\overline{\mathbf{R}}_x^\perp)^T, \quad (44)$$

$$\psi^\perp = \sum_{i=I+1}^M \left(\mathbf{q}^{(i)} \otimes (\mathbf{P}_x^\perp \mathbf{q}^{(i)})^* \right). \quad (45)$$

C. Direct optimization of source-wise CBF

Before deriving the optimization with the source-wise factorization, we show that we can directly optimize the source-wise CBF in Eq. (12), and summarize its characteristics. With this setting, the CBF and the objective are both defined separately for each source in Eqs. (12) and (17), and thus, the optimization can be performed separately for each source. The resultant algorithm is, therefore, identical to that proposed for DN+DR in [39].

For presenting the solution, we introduce the following vector representation of Eq. (12).

$$\mathbf{y}_t^{(i)} = (\underline{\mathbf{w}}^{(i)})^H \underline{\mathbf{x}}_t, \quad (46)$$

where $\underline{\mathbf{w}}^{(i)}$ is defined, using Eq. (13), as

$$\underline{\mathbf{w}}^{(i)} = \left[(\mathbf{w}_0^{(i)})^T, (\overline{\mathbf{w}}^{(i)})^T \right]^T, \quad (47)$$

Then, when $\lambda_t^{(i)}$ and $\tilde{\mathbf{v}}^{(i)}$ are given, Eq. (17) becomes a simple constraint quadratic form as

$$\mathcal{L}_w(\underline{\mathbf{w}}^{(i)}) = \left\| \underline{\mathbf{w}}^{(i)} \right\|_{\overline{\mathbf{R}}_x^{(i)}}^2 \quad \text{s.t.} \quad (\underline{\mathbf{w}}^{(i)})^H \underline{\mathbf{v}}^{(i)} = 1, \quad (48)$$

where $\overline{\mathbf{R}}_x^{(i)}$ is the covariance matrix defined in Eq. (26), and $\underline{\mathbf{v}}^{(i)} = \left[(\tilde{\mathbf{v}}^{(i)})^T, 0, \dots, 0 \right]^T \in \mathbb{C}^{M(L-\Delta+1) \times 1}$ corresponds to the RTF $\tilde{\mathbf{v}}^{(i)}$ with zero padding. Finally, the solution is given as

$$\underline{\mathbf{w}}^{(i)} = \frac{(\overline{\mathbf{R}}_x^{(i)})^{-1} \underline{\mathbf{v}}^{(i)}}{(\underline{\mathbf{v}}^{(i)})^H (\overline{\mathbf{R}}_x^{(i)})^{-1} \underline{\mathbf{v}}^{(i)}}. \quad (49)$$

An advantage of the solution using the source-wise CBF is that it can be obtained by a closed form equation provided the RTF and the time-varying variance of the desired signal are given, and we do not need to consider the interaction between DN and DR. With this approach, however, it is necessary to estimate the RTF directly from a reverberant observation similar to [24]. A solution to this problem is to use dereverberation preprocessing based on a WPE filter for the RTF estimation. It was shown in [30] that the output of a WPE filter can be obtained in a computationally efficient way within the framework of this approach. However, the source-wise factorization approach described in the following can more naturally solve this problem. So, this paper adopts it as the solution.

D. Optimization based on source-wise factorization

With the source-wise factorization, similar to the case with the direct optimization of the source-wise CBF, the optimization can be performed separately for each source, and the resultant algorithm is identical to that proposed for DN+DR in [31]. Considering that a CBF can be written based on Eqs. (14) and (15) as $y_t^{(i)} = (\mathbf{q}^{(i)})^H \left(\mathbf{x}_t - (\overline{\mathbf{G}}^{(i)})^H \overline{\mathbf{x}}_t \right)$ and using the factorized form of $\mathbf{R}_{\mathbf{x}}^{(i)}$ in Eq. (26), the objective in Eq. (17) can be rewritten as

$$\begin{aligned} \mathcal{L}_i \left(\overline{\mathbf{G}}^{(i)}, \mathbf{q}^{(i)} \right) = & \left\| \left(\overline{\mathbf{G}}^{(i)} - \left(\overline{\mathbf{R}}_{\mathbf{x}}^{(i)} \right)^{-1} \mathbf{P}_{\mathbf{x}}^{(i)} \right) \mathbf{q}^{(i)} \right\|_{\overline{\mathbf{R}}_{\mathbf{x}}^{(i)}}^2 \\ & + \left\| \mathbf{q}^{(i)} \right\|_{\left(\overline{\mathbf{R}}_{\mathbf{x}}^{(i)} - \left(\mathbf{P}_{\mathbf{x}}^{(i)} \right)^H \left(\overline{\mathbf{R}}_{\mathbf{x}}^{(i)} \right)^{-1} \mathbf{P}_{\mathbf{x}}^{(i)} \right)}^2. \end{aligned} \quad (50)$$

In the above objective, $\overline{\mathbf{G}}^{(i)}$ is contained only in the first term, and the term can be minimized, not depending on the value of $\mathbf{q}^{(i)}$, when $\overline{\mathbf{G}}^{(i)}$ takes the following value.

$$\overline{\mathbf{G}}^{(i)} = \left(\overline{\mathbf{R}}_{\mathbf{x}}^{(i)} \right)^{-1} \mathbf{P}_{\mathbf{x}}^{(i)}. \quad (51)$$

So, this is a solution⁶ of $\overline{\mathbf{G}}^{(i)}$ that globally minimizes the objective given the time-varying variance $\lambda_t^{(i)}$. Interestingly, this solution is identical to that of the conventional WPE dereverberation. This means that the WPE filter optimized solely for dereverberation can perform the optimal dereverberation for the joint optimization not depending on the subsequent beamforming, provided the time-varying variance of the desired source is given for the optimization. In addition, unlike the source-packed factorization approach, this approach does not need to compensate for the rank deficiency of the covariance matrix. We refer to this filter $\overline{\mathbf{G}}^{(i)}$ as a single-target WPE filter in this paper.

Once $\overline{\mathbf{G}}^{(i)}$ is obtained as the above solution, the objective in Eq. (17) can be rewritten as

$$\mathcal{L}_i \left(\mathbf{q}^{(i)} \right) = \left\| \mathbf{q}^{(i)} \right\|_{\overline{\mathbf{R}}_{\mathbf{z}}^{(i)}}^2 \quad \text{s.t.} \quad \left(\mathbf{q}^{(i)} \right)^H \tilde{\mathbf{v}}^{(i)} = 1, \quad (52)$$

⁶This is not a unique solution. The first term is minimized even when an arbitrary matrix, of which null space includes $\mathbf{q}^{(i)}$, is added to Eq. (51).

where $\overline{\mathbf{R}}_{\mathbf{z}}^{(i)}$ is a variance-normalized covariance matrix of the output of the single-target WPE filter, calculated as

$$\overline{\mathbf{R}}_{\mathbf{z}}^{(i)} = \frac{1}{T} \sum_{t=1}^T \frac{\mathbf{z}_t^{(i)} \left(\mathbf{z}_t^{(i)} \right)^H}{\lambda_t^{(i)}} \in \mathbb{C}^{M \times M}. \quad (53)$$

Then, the solution can be obtained, under the distortionless constraint, as a wMPDR beamformer defined by

$$\mathbf{q}^{(i)} = \frac{\left(\overline{\mathbf{R}}_{\mathbf{z}}^{(i)} \right)^{-1} \tilde{\mathbf{v}}^{(i)}}{\left(\tilde{\mathbf{v}}^{(i)} \right)^H \left(\overline{\mathbf{R}}_{\mathbf{z}}^{(i)} \right)^{-1} \tilde{\mathbf{v}}^{(i)}}. \quad (54)$$

Eqs. (52) to (54) are very similar to Eqs. (38) to (40), and the difference is whether the dereverberation is performed by multiple-target WPE filter or single-target WPE filter.

With the source-wise factorization, the solution can be obtained in a closed form way when $\lambda_t^{(i)}$ and $\tilde{\mathbf{v}}^{(i)}$ are given, similar to the case with the direct optimization of the source-wise CBF. In addition, the output of the WPE filter is obtained as $\mathbf{z}_t^{(i)}$ in Eq. (14), and can be efficiently used for estimation of the RTFs. Furthermore, the size of the temporal-spatial covariance matrix in Eq. (29) is much smaller than that in Eq. (36) of the source-packed factorization, and thus the computational cost can be small. (See Section IV for more detailed discussion on the computing cost.)

E. Processing flow with estimation of $\lambda_t^{(i)}$ and $\tilde{\mathbf{v}}^{(i)}$

Algorithms 1 and 2, respectively, describe examples of processing flows for source-packed and source-wise factorization-based optimization of a CBF, including the estimation of the time-varying variances, $\lambda_t^{(i)}$, and the RTFs, $\tilde{\mathbf{v}}^{(i)}$. Hereafter, we refer to both algorithms as A-1 and A-2 for brevity. While A-1 estimates all the sources, $y_t^{(i)}$ for all i , at the same time from the observed signal \mathbf{x}_t , A-2 estimates only one of the sources, $y_t^{(i)}$ for a certain i , and (if necessary) is repeatedly applied to the observed signal to estimate all the sources one after another. As auxiliary inputs, TF masks are provided for both algorithms. A TF mask $\gamma_t^{(i)}$ is associated with a source and a TF point, takes a value between 0 and 1, and indicates whether the desired signal of the source dominates the TF point ($\gamma_t^{(i)} = 1$) or not ($\gamma_t^{(i)} = 0$). The TF masks over all the TF points are used to estimate the RTF(s) of the desired signal(s) in line 19 of A-1 and line 7 of A-2. (See Section III-E1 for the detail of estimation of the TF masks and the RTFs.)

Both algorithms estimate the time-varying variances $\lambda_t^{(i)}$ based on the same objective as that for the CBF, defined in Eq. (17). Because a closed form solution to the estimation of the CBF and the time-varying variances is not known, an iterative and alternate optimization scheme is introduced to both algorithms. In each iteration, the time-varying variances, $\lambda_t^{(i)}$, are updated in line 23 of A-1 and line 11 of A-2 as the power of the previously estimated values of the desired signal $y_t^{(i)}$, and then the CBF and the desired signal $y_t^{(i)}$ are updated while fixing the time-varying variances. The iteration is repeated until convergence is obtained.

Algorithm 1: Source-packed factorization-based optimization for estimation of all the sources.

Data: Observed signal \mathbf{x}_t for all t
 TF masks $\gamma_t^{(i)}$ for all t and $1 \leq i \leq I$
Result: Estimated sources $y_t^{(i)}$ for all t and $1 \leq i \leq I$

- 1 Initialize $\lambda_t^{(i)}$ as $\|\mathbf{x}_t\|_{\mathbf{I}_M}^2/M$ for all t and $1 \leq i \leq I$
- 2 Initialize $\mathbf{q}^{(i)}$ as the i th column of \mathbf{I}_M for $1 \leq i \leq I$
- 3 Initialize \mathbf{z}_t as \mathbf{x}_t for all t
- 4 **repeat**
- 5 $\overline{\mathbf{R}}_{\mathbf{x}}^{(i)} \leftarrow \frac{1}{T} \sum_{t=1}^T \frac{\overline{\mathbf{x}}_t \overline{\mathbf{x}}_t^H}{\lambda_t^{(i)}}$ for $1 \leq i \leq I$
- 6 $\mathbf{P}_{\mathbf{x}}^{(i)} \leftarrow \frac{1}{T} \sum_{t=1}^T \frac{\overline{\mathbf{x}}_t \overline{\mathbf{x}}_t^H}{\lambda_t^{(i)}}$ for $1 \leq i \leq I$
- 7 $\Psi \leftarrow \sum_{i=1}^I \left(\mathbf{q}^{(i)} (\mathbf{q}^{(i)})^H \otimes \left(\overline{\mathbf{R}}_{\mathbf{x}}^{(i)} \right)^T \right)$
- 8 $\psi \leftarrow \sum_{i=1}^I \left(\mathbf{q}^{(i)} \otimes \left(\mathbf{P}_{\mathbf{x}}^{(i)} \mathbf{q}^{(i)} \right)^* \right)$
- 9 **Begin** Add orthogonal complement beamformer
- 10 Set $\mathbf{q}^{(I+1)}, \dots, \mathbf{q}^{(M)}$ be orthonormal bases for the orthogonal complement \mathbf{Q}^\perp of \mathbf{Q}
- 11 $\lambda_t^\perp \leftarrow \left| \left(\sum_{i=I+1}^M \mathbf{q}^{(i)} \right)^H \mathbf{z}_t \right|^2$
- 12 $\overline{\mathbf{R}}_{\mathbf{x}}^\perp \leftarrow \frac{1}{T} \sum_{t=1}^T \frac{\overline{\mathbf{x}}_t \overline{\mathbf{x}}_t^H}{\lambda_t^\perp}$
- 13 $\mathbf{P}_{\mathbf{x}}^\perp \leftarrow \frac{1}{T} \sum_{t=1}^T \frac{\overline{\mathbf{x}}_t \overline{\mathbf{x}}_t^H}{\lambda_t^\perp}$
- 14 $\Psi \leftarrow \Psi + \left(\sum_{i=I+1}^M \mathbf{q}^{(i)} (\mathbf{q}^{(i)})^H \right) \otimes \left(\overline{\mathbf{R}}_{\mathbf{x}}^\perp \right)^T$
- 15 $\psi \leftarrow \psi + \sum_{i=I+1}^M \left(\mathbf{q}^{(i)} \otimes \left(\mathbf{P}_{\mathbf{x}}^\perp \mathbf{q}^{(i)} \right)^* \right)$
- 16 **End**
- 17 $\overline{\mathbf{g}} \leftarrow \Psi^+ \psi$
- 18 $\mathbf{z}_t \leftarrow \mathbf{x}_t - \overline{\mathbf{X}}_t \overline{\mathbf{g}}$
- 19 Estimate $\tilde{\mathbf{v}}^{(i)}$ based on \mathbf{z}_t and $\gamma_t^{(i)}$ for $1 \leq i \leq I$
- 20 $\mathbf{R}_{\mathbf{z}}^{(i)} \leftarrow \frac{1}{T} \sum_{t=1}^T \frac{\mathbf{z}_t (\mathbf{z}_t)^H}{\lambda_t^{(i)}}$ for $1 \leq i \leq I$
- 21 $\mathbf{q}^{(i)} \leftarrow \frac{(\mathbf{R}_{\mathbf{z}}^{(i)})^+ \tilde{\mathbf{v}}^{(i)}}{(\tilde{\mathbf{v}}^{(i)})^H (\mathbf{R}_{\mathbf{z}}^{(i)})^+ \tilde{\mathbf{v}}^{(i)}}$ for $1 \leq i \leq I$
- 22 $y_t^{(i)} \leftarrow (\mathbf{q}^{(i)})^H \mathbf{z}_t$ for $1 \leq i \leq I$
- 23 $\lambda_t^{(i)} \leftarrow |y_t^{(i)}|^2$ for $1 \leq i \leq I$
- 24 **until convergence**

The optimization methods described in Sections III-B and III-D are used in respective algorithms for update of the CBF and the desired signal(s). The WPE filter is first estimated in lines 5 to 17 of A-1 and lines 3 to 5 of A-2, and applied in line 18 of A-1 and line 6 of A-2. After the RTF(s) is updated using the dereverberated signals, the wMPDR beamformer is estimated in lines 20 and 21 of A-1 and lines 8 and 9 of A-2, and applied in line 22 of A-1 and line 10 of A-2.

Figure 2 illustrates the processing flow of a CBF with the source-wise factorization for estimating a source i .

1) *Methods for estimating TF masks and RTFs:* In experiments, for estimating TF masks, $\gamma_t^{(i)}$, for all i and t , we used a frequency-domain Convolutional Neural Network trained using utterance-level Permutation Invariant Training criterion (CNN-uPIT) [41]. According to our preliminary experiments [32], we set the network structure as a CNN with a large

Algorithm 2: Source-wise factorization-based optimization for estimation of the i th source

Data: Observed signal \mathbf{x}_t for all t
 TF masks $\gamma_t^{(i)}$ for all t
Result: Estimated i th source $y_t^{(i)}$ for all t

- 1 Initialize $\lambda_t^{(i)}$ as $\|\mathbf{x}_t\|_{\mathbf{I}_M}^2/M$ for all t
- 2 **repeat**
- 3 $\overline{\mathbf{R}}_{\mathbf{x}}^{(i)} \leftarrow \frac{1}{T} \sum_{t=1}^T \frac{\overline{\mathbf{x}}_t \overline{\mathbf{x}}_t^H}{\lambda_t^{(i)}}$
- 4 $\mathbf{P}_{\mathbf{x}}^{(i)} \leftarrow \frac{1}{T} \sum_{t=1}^T \frac{\overline{\mathbf{x}}_t \overline{\mathbf{x}}_t^H}{\lambda_t^{(i)}}$
- 5 $\overline{\mathbf{G}}^{(i)} \leftarrow \left(\overline{\mathbf{R}}_{\mathbf{x}}^{(i)} \right)^+ \mathbf{P}_{\mathbf{x}}^{(i)}$
- 6 $\mathbf{z}_t^{(i)} \leftarrow \mathbf{x}_t - \left(\overline{\mathbf{G}}^{(i)} \right)^H \overline{\mathbf{x}}_t$
- 7 Estimate $\tilde{\mathbf{v}}^{(i)}$ based on $\mathbf{z}_t^{(i)}$ and $\gamma_t^{(i)}$
- 8 $\hat{\mathbf{R}}_{\mathbf{z}}^{(i)} \leftarrow \frac{1}{T} \sum_{t=1}^T \frac{\mathbf{z}_t^{(i)} (\mathbf{z}_t^{(i)})^H}{\lambda_t^{(i)}}$
- 9 $\mathbf{q}^{(i)} \leftarrow \frac{(\hat{\mathbf{R}}_{\mathbf{z}}^{(i)})^+ \tilde{\mathbf{v}}^{(i)}}{(\tilde{\mathbf{v}}^{(i)})^H (\hat{\mathbf{R}}_{\mathbf{z}}^{(i)})^+ \tilde{\mathbf{v}}^{(i)}}$
- 10 $y_t^{(i)} \leftarrow (\mathbf{q}^{(i)})^H \mathbf{z}_t^{(i)}$
- 11 $\lambda_t^{(i)} \leftarrow |y_t^{(i)}|^2$
- 12 **until convergence**

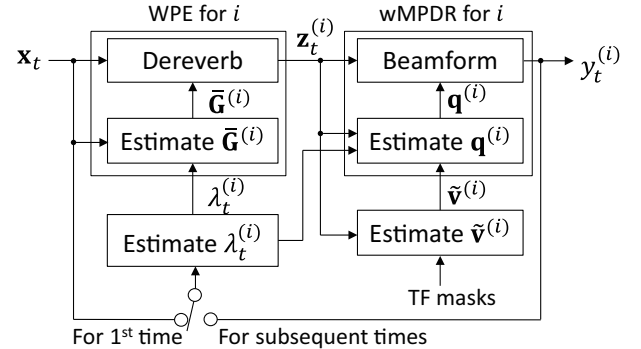


Fig. 2. Processing flow of source-wise factorization-based CBF for estimating a source i .

receptive field similar to one used by a fully-Convolutional Time-domain Audio Separation Network (Conv-TasNet) [42]. The network was trained so that it receives the output of the WPE filter that is obtained at the first iteration in the iterative optimization of the CBF, and estimates the TF masks of the desired signals. The input of the network was set as concatenation of the real and imaginary parts of STFT coefficients, and the loss function was set as the (scale-dependent) signal-to-distortion ratio (SDR) of the enhanced signal obtained by multiplying the estimated masks to the observed signal. For the training and validation data, we synthesized mixtures using two utterances randomly extracted from the WSJ-CAM0 corpus [43] and two room impulse responses and background noise extracted from the REVERB Challenge training set [18].

For the estimation of the RTFs, $\tilde{\mathbf{v}}^{(i)}$, we adopt a method based on eigenvalue decomposition with noise covariance

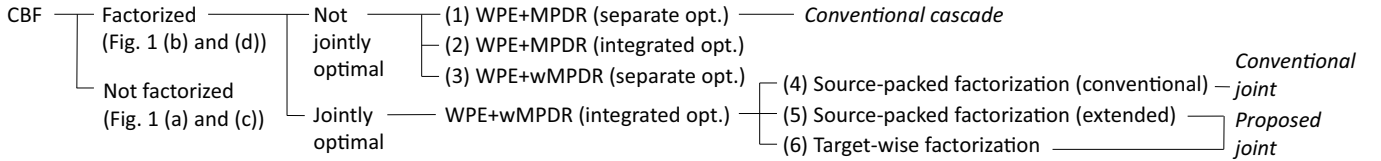


Fig. 3. Tree diagram of CBFs used in experiments. (1) and (4) are conventional cascade configuration and conventional joint optimization approaches, (5) and (6) are proposed methods, and (2) and (3) are used just for comparison. See Fig. 4 for the difference between separate and integrated optimization.

whitening [44], [45]. With this technique, the steering vector $\mathbf{v}^{(i)}$ is first estimated as

$$\mathbf{v}^{(i)} = \mathcal{R}_{\setminus i} \text{MaxEig} \left(\mathcal{R}_{\setminus i}^{-1} \mathcal{R}_i \right), \quad (55)$$

where $\text{MaxEig}(\cdot)$ is a function that calculates the eigenvector corresponding to the maximum eigenvalue, \mathcal{R}_i and $\mathcal{R}_{\setminus i}$ are a spatial covariance matrix of the i -th desired signal and that of the other signals, respectively, estimated as

$$\mathcal{R}_i = \frac{\sum_t \gamma_t^{(i)} \mathbf{z}_t^{(i)} \left(\mathbf{z}_t^{(i)} \right)^H}{\sum_t \gamma_t^{(i)}}, \quad (56)$$

$$\mathcal{R}_{\setminus i} = \frac{\sum_t \left(1 - \gamma_t^{(i)} \right) \mathbf{z}_t^{(i)} \left(\mathbf{z}_t^{(i)} \right)^H}{\sum_t \left(1 - \gamma_t^{(i)} \right)}. \quad (57)$$

Then, the RTF is obtained by Eq. (4).

IV. DISCUSSION

In summary, the proposed techniques can perform joint optimization for DN+DR+SS with greatly reduced computing cost in comparison with the direct application of the conventional joint optimization technique proposed for DR+SS to DN+DR+SS. With the source-packed factorization, because the optimization of $\overline{\mathbf{G}}$ is dependent on \mathbf{Q} , it is necessary to calculate the huge covariance matrix Ψ , making the computing cost of the conventional joint optimization technique extremely high. In contrast, the proposed extension of this approach greatly reduces the size of the matrix to be calculated substantively from $M^2(L - \Delta)$ for Ψ to $M(L - \Delta)$ for $\overline{\mathbf{R}}_{\mathbf{x}}$. On the other hand, with the source-wise factorization, $\overline{\mathbf{G}}^{(i)}$ can be optimized independently of $\mathbf{q}^{(i)}$, which also allows us to reduce the size of the matrix to be calculated to the same as that of the above extension. Furthermore, we can skip calculation of the additional matrix, $\overline{\mathbf{R}}_{\mathbf{x}}^{\perp}$, which is required for the source-packed factorization. This makes the source-wise factorization approach computationally further efficient. A drawback of the source-wise factorization is that it has to handle I -times larger number of dereverberated signals than the source-packed factorization has to.

The source-wise factorization approach has additional benefits when it is used in specific scenarios listed below:

- The source-wise factorization approach can estimate the CBF by a closed-form equation when time-varying source variances are given, or estimated, e.g., using neural networks [15], [12]. In such a case, we can skip the iterative optimization, resulting in further reduction of the computing cost. In contrast, the source-packed factorization

approach needs to maintain iterations to estimate \mathbf{Q} and $\overline{\mathbf{G}}$ alternately due to their dependency.

- The above scheme can be advantageous when it is combined with neural network-based target speaker extraction that has been actively studied recently [13]. With this combination, the target source can be estimated using the closed form equation while skipping the estimation of other sources.

In addition, the source-wise factorization can be used as a versatile technique for optimizing a CBF. For example, [28] shows an example application of the approach to the blind signal processing for DR+SS. With this application, the optimization becomes computationally much less demanding than the conventional approach without loss of optimality.

V. EXPERIMENTS

This section experimentally confirms the effectiveness of the proposed joint optimization approaches. Figure 3 summarizes optimization methods to be evaluated in the experiments (See Sections V-C and V-D for the detail of the methods). We compare them in the following two aspects.

1) Effectiveness of joint optimization

We compare a CBF with and without joint optimization in terms of estimation accuracy. The source-wise factorization approach (Fig. 3 (6)) is compared with the conventional cascade configuration (Fig. 3 (1)), and two additional test conditions (Fig. 3 (2) and (3)).

2) Comparison among joint optimization approaches

We compare three joint optimization approaches, i.e., the source-packed factorization approach with its conventional setting (Fig. 3 (4)), its proposed extension (Fig. 3 (5)), and the source-wise factorization approach (Fig. 3 (6)), described, respectively, in Sections III-B1, III-B2, and III-D, in terms of computational efficiency and estimation accuracy.

A. Dataset and evaluation metrics

For the evaluation, we prepared for a set of noisy reverberant speech mixtures (REVERB-MIX) using the REVERB Challenge dataset (REVERB) [18]. Each utterance in REVERB contains a single reverberant speech with moderate stationary diffuse noise. For generating a set of test data, we mixed two utterances extracted from REVERB, one from its development set (Dev set) and the other from its evaluation set (Eval set), so that each pair of mixed utterances were recorded in the same room, by the same microphone array, and under the same condition (near or far, RealData or SimData). We categorize

TABLE I
BEAMFORMER CONFIGURATIONS USED IN EXPERIMENTS

	M	L at each freq. range (kHz)			I	#iterations
		0.0-0.8	0.8-1.5	1.5-8.0		
Config-1	8	20	16	8	2	10
Config-2	4	20	16	8	2	10

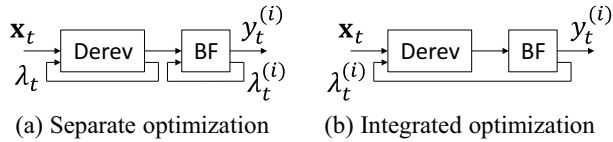


Fig. 4. Separate and integrated optimization schemes. In the separate optimization, λ_t for Derev is the same for all the sources.

the test data according to the original categories of the data in REVERB (e.g., SimData or RealData). We created the same number of mixtures in the test data as in the REVERB Eval set, such that each utterance in the REVERB Eval set is contained in one of the mixtures in the test data. Furthermore, the length of each mixture in the test data was set at the same as that of the corresponding utterance in the REVERB Eval set.

In the experiments, we estimated two speech signals from each mixture, and evaluated only one of them corresponding to the REVERB Eval set, using baseline evaluation tools prepared for it. We selected the signal to be evaluated from the two estimated speech signals based on the correlation between the separated signals and the original signal in the REVERB Eval set. As objective measures for speech enhancement [46], we used the Cepstrum Distance (CD), the Frequency-Weighted Segmental SNR (FWSSNR), and the Perceptual Evaluation of Speech Quality (PESQ). To evaluate the ASR performance, we used a baseline ASR system for REVERB that was recently developed using Kaldi [47]. This system is composed of a Time-Delay Neural Network (TDNN) acoustic model trained using lattice-free maximum mutual information (LF-MMI) and online i-vector extraction, and a trigram language model. They are trained on the REVERB training set.

B. Configurations of CBF

Table I summarizes two configurations of the CBF examined in experiments including the number of microphones M , the filter length L , the number of sources I , and the number of optimization iterations. The sampling frequency was 16 kHz. A Hann window was used for a short-time analysis with the frame length and shift being set at 32 ms and 8 ms, respectively. The prediction delay was set at $\Delta = 4$ for the WPE filter.

In the iterative optimization, the time-varying variances of sources were initialized as those of the observed signal for the WPE filter and as 1 for the wMPDR beamformer for all the methods.

C. Experiment-1: effectiveness of joint optimization

In this experiment, we evaluated the effectiveness of the joint optimization focusing on its two characteristics. First,

TABLE II
WER (%) FOR REALDATA AND CD (dB), FWSSNR (dB), AND PESQ FOR SIMDATA IN REVERB-MIX OBTAINED USING DIFFERENT BEAMFORMERS AFTER FIVE ITERATIONS WITH CONFIG-1. SCORES FOR REVERB-MIX AND REVERB (I.E., SINGLE SPEAKER) WITHOUT ENHANCEMENT ARE ALSO SHOWN.

Beamformer	WER	CD	FWSSNR	PESQ
Observed (REVERB-MIX)	62.49	5.44	1.12	1.12
Single speaker (REVERB)	18.61	3.97	3.62	1.48
MPDR (w/o iteration)	30.79	4.40	3.07	1.45
wMPDR	28.75	3.96	4.46	1.60
(1) WPE+MPDR (separate)	23.04	4.30	3.77	1.58
(2) WPE+MPDR (integrated)	23.22	4.28	3.66	1.56
(3) WPE+wMPDR (separate)	21.53	3.74	5.42	1.77
(6) WPE+wMPDR (integrated)	20.04	3.67	5.57	1.80

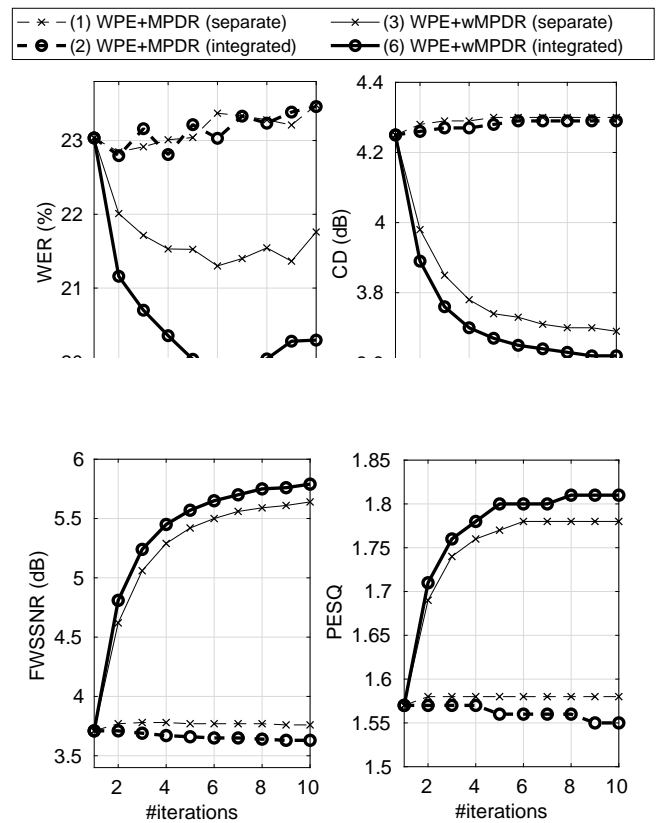


Fig. 5. Comparison among joint optimization and cascade configuration approaches when using WPE+MPDR and WPE+wMPDR with integrated and separate optimization schemes using Config-1.

we compared two different filter combinations, one composed of a WPE filter followed by a wMPDR beamformer (WPE+wMPDR) and the other composed of a WPE filter followed by an MPDR beamformer (WPE+MPDR). The former is required for the joint optimization, and the latter has been used for the conventional cascade configuration. Second, we compared two different optimization schemes shown in Fig. 4, namely “separate optimization” and “integrated optimization” schemes. With the separate optimization, the iterative estimation of the time-varying variance was performed separately for the WPE filter and for the beamformer. This is the scheme

used by the conventional cascade configuration. In contrast with the integrated optimization, the iterative estimation was performed jointly for the WPE filter and the beamformer. A significant difference between the two schemes is whether the WPE filter uses time-varying variances of individual sources estimated by the beamformer.

Table II compares WERs, CDs, FWSSNRs, and PESQs obtained after five iterations using two beamformers, MPDR and wMPDR, (1) the conventional cascade configuration approach (2) and (3) for two test conditions, and (6) the source-wise factorization-based joint optimization approach, all performed using configuration Config-1 in Table I. The table shows: 1) WPE+MPDR and WPE+wMPDR greatly outperformed MPDR and wMPDR, respectively, with all the conditions 2) the joint optimization approach, i.e., (6) WPE+wMPDR with the integrated optimization, substantially outperformed all the other methods in terms of all the measures. Furthermore Fig. 5 shows convergence curves of the cascade configuration approach, two test conditions, and the joint optimization approach. The performance of (6) joint optimization approach improved as the number of iterations increased, confirming the usefulness of the iterative estimation of the time-varying variances. In contrast, (1) and (2) for WPE+MPDR did not improve the performance after the first iteration with both integrated and separate optimization schemes.

The above results clearly show that the two characteristics of the joint optimization approach, i.e., the optimal combination of a WPE filter and a wMPDR beamformer and the integrated optimization for estimating the source variances, are both very effective for improving the performance.

D. Experiment-2: Comparison among joint optimization approaches

In this experiments, we compared three joint optimization approaches, namely two source-packed factorization approaches, respectively, described in Sections III-B1 and III-B2, and denoted as “(4) Source-packed factorization (conventional)” and “(5) Source-packed factorization (extended),” and the source-wise factorization approach, denoted as “(6) Source-wise factorization.” (4) Source-packed factorization (conventional) corresponds to the conventional joint optimization technique, and (5) Source-packed factorization (extended) and (6) Source-wise factorization correspond to our proposed methods. Figure 6 compares the WERs obtained using the three approaches with Config-1 and Config-2. It shows that the proposed methods, i.e., (5) Source-packed factorization (extended) and (6) Source-wise factorization, performed comparably well and both greatly outperformed (4) Source-packed factorization (conventional).

Table III compares computing times required for the three approaches to perform ten iterations for processing a mixture utterance with the length being 9.44 s. The computing time was measured by a Matlab interpreter as the elapsed time. As shown in the table, for both configurations, (5) Source-packed factorization (extended) greatly reduced the computing time in comparison with (4) Source-packed factorization (conventional), and (6) Source-wise factorization further reduced the computing time.

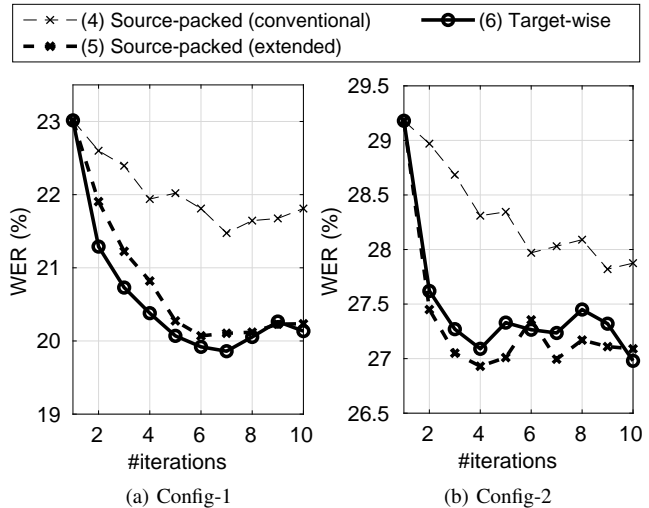


Fig. 6. WERs (%) obtained when jointly optimizing WPE+wMPDR based on the source-packed factorization (conventional/extended) and source-wise factorization approaches.

TABLE III
COMPUTING TIME REQUIRED FOR PROCESSING A MIXTURE UTTERANCE WITH LENGTH OF 9.44 s. THE COMPUTING TIME WAS MEASURED BY ELAPSED TIME ON A MATLAB INTERPRETER.

Method	Time (s)	
	Config-1	Config-2
(4) Source-packed factorization (conventional)	3467	688
(5) Source-packed factorization (extended)	209	33
(6) Source-wise factorization	40	23

The above results clearly demonstrate the superiority of the two proposed approaches over the conventional joint optimization technique in terms of both computational efficiency and estimation accuracy. However, Table III indicates that the proposed approaches still require relatively large computing cost to obtain high performance gain shown in Fig. 6 (a). Future work should include solving this problem. For example, it might be mitigated when we set the goal as extraction of a single target source. Then, thanks to the characteristics of the source-wise factorization, we can skip the estimation of the other sources, and skip the iterative estimation using source variances separately estimated, e.g., by a neural network. As a reference, the computing time, 40 s, in Table III required for the source-wise factorization with Config-1 roughly corresponds to 2.0 s for one iteration per source (namely 40 s/10/2), which results in the real-time factor being 0.21 (= 2.0 s/9.44 s).

VI. CONCLUDING REMARKS

This paper presented methods for optimizing a CBF that performs DN+DR+SS based on the ML estimation. We introduced two different approaches for factorizing a CBF, i.e., source-packed and source-wise factorization approaches, and derived the optimization algorithms for respective approaches. It was shown that a CBF can be factorized without loss of optimality into a multiple-target WPE filter followed by wMPDR beamformers using the source-packed factorization approach, and into a set of single-target WPE filters followed

by wMPDR beamformers using the source-wise factorization approach. This paper also presented overall processing flows for both approaches on an assumption that TF masks are provided as auxiliary inputs. In the flows, the time varying source variances, which are required for the ML estimation, can be optimally estimated jointly with the CBF using iterative optimization, and steering vectors of the desired signals, which are required for beamformer optimization, can be reliably estimated based on the dereverberated multichannel signals obtained at a step of the optimization.

Experiments using noisy reverberant sound mixtures show that the proposed optimization approaches substantially improve the performance of the CBF in comparison with the conventional cascade configuration in terms of ASR performance and reduction of signal distortion. It is also shown that the proposed approaches can greatly reduce the computing cost with improved estimation accuracy in comparison with the conventional joint optimization technique. The proposed approaches, however, still result in relatively large computing costs to obtain high performance gain. The solution to this problem should be included in the future work.

APPENDIX A

DERIVATION OF EQS. (41) AND (42)

We can rewrite Ψ in Eq. (36) using Eq. (34) as

$$\Psi = \frac{1}{T} \sum_t \bar{\mathbf{x}}_t^H \Phi_{\mathbf{q},t} \bar{\mathbf{x}}_t, \quad (58)$$

$$= \frac{1}{T} \sum_t \sum_i \frac{1}{\lambda_t^{(i)}} \left(\left(\mathbf{q}^{(i)} \right)^H \bar{\mathbf{x}}_t \right)^H \left(\left(\mathbf{q}^{(i)} \right)^H \bar{\mathbf{x}}_t \right). \quad (59)$$

Using Eq. (31), $\left(\mathbf{q}^{(i)} \right)^H \bar{\mathbf{x}}_t$ can further be rewritten as

$$\left(\mathbf{q}^{(i)} \right)^H \bar{\mathbf{x}}_t = \left(\mathbf{q}^{(i)} \right)^H \left(\mathbf{I}_M \otimes \bar{\mathbf{x}}_t^T \right), \quad (60)$$

$$= \left(\mathbf{q}^{(i)} \right)^H \otimes \bar{\mathbf{x}}_t^T. \quad (61)$$

Substituting the above equation in Eq. (59) yields

$$\Psi = \frac{1}{T} \sum_t \sum_i \frac{1}{\lambda_t^{(i)}} \left(\mathbf{q}^{(i)} \otimes \left(\bar{\mathbf{x}}_t^H \right)^T \right) \left(\left(\mathbf{q}^{(i)} \right)^H \otimes \bar{\mathbf{x}}_t^T \right), \quad (62)$$

$$= \frac{1}{T} \sum_t \sum_i \frac{1}{\lambda_t^{(i)}} \left(\mathbf{q}^{(i)} \left(\mathbf{q}^{(i)} \right)^H \right) \otimes \left(\bar{\mathbf{x}}_t \bar{\mathbf{x}}_t^H \right)^T, \quad (63)$$

$$= \sum_i \left(\mathbf{q}^{(i)} \left(\mathbf{q}^{(i)} \right)^H \right) \otimes \left(\bar{\mathbf{R}}_x^{(i)} \right)^T. \quad (64)$$

Similarly, we can obtain

$$\psi = \frac{1}{T} \sum_t \bar{\mathbf{x}}_t^H \Phi_{\mathbf{q}} \mathbf{x}_t, \quad (65)$$

$$= \frac{1}{T} \sum_t \sum_i \frac{1}{\lambda_t^{(i)}} \left(\mathbf{q}^{(i)} \otimes \left(\bar{\mathbf{x}}_t^H \right)^T \right) \left(\left(\mathbf{q}^{(i)} \right)^H \mathbf{x}_t \right), \quad (66)$$

$$= \frac{1}{T} \sum_t \sum_i \frac{1}{\lambda_t^{(i)}} \left(\mathbf{q}^{(i)} \otimes \left(\left(\mathbf{x}_t \bar{\mathbf{x}}_t^H \right)^T \left(\mathbf{q}^{(i)} \right)^* \right) \right), \quad (67)$$

$$= \sum_i \left(\mathbf{q}^{(i)} \otimes \left(\mathbf{P}_x^{(i)} \mathbf{q}^{(i)} \right)^* \right). \quad (68)$$

REFERENCES

- [1] B. D. V. Veen and K. M. Buckley, "Beamforming: A versatile approach to spatial filtering," *IEEE ASSP Magazine*, vol. 5, no. 2, pp. 4–24, 1988.
- [2] H. L. V. Trees, *Optimum Array Processing, Part IV of Detection, Estimation, and Modulation Theory*. New York: Wiley-Interscience, 2002.
- [3] H. Cox, "Resolving power and sensitivity to mismatch of optimum array processors," *The Journal of the Acoustical Society of America*, vol. 54, pp. 771–785, 1973.
- [4] M. Souden, J. Benesty, and S. Affes, "On optimal frequency-domain multichannel linear filtering for noise reduction," *IEEE Trans. Audio, Speech, and Language Processing*, vol. 18, no. 2, pp. 260–276, 2007.
- [5] A. Hyvärinen, J. Karhunen, and E. Oja, *Independent Component Analysis*. New York: John Wiley & Sons, 2001.
- [6] T. Kim, H. T. Attias, S.-Y. Lee, and T.-W. Lee, "Blind source separation exploiting higher-order frequency dependencies," *IEEE Trans. on Speech, and Audio Processing*, vol. 15, no. 1, pp. 70–79, 2006.
- [7] M. Souden, S. Araki, K. Kinoshita, T. Nakatani, and H. Sawada, "A multichannel MMSE-based framework for speech source separation and noise reduction," *IEEE Trans on Audio, Speech, and Language Processing*, vol. 21, no. 9, pp. 1913–1928, 2010.
- [8] T. Nakatani, T. Yoshioka, K. Kinoshita, M. Miyoshi, and B.-H. Juang, "Speech dereverberation based on variance-normalized delayed linear prediction," *IEEE Transactions on Audio, Speech, and Language Processing*, vol. 18, no. 7, pp. 1717–1731, 2010.
- [9] T. Yoshioka and T. Nakatani, "Generalization of multi-channel linear prediction methods for blind MIMO impulse response shortening," *IEEE Transactions on Audio, Speech and Language Processing*, vol. 20, no. 10, pp. 2707–2720, 2012.
- [10] A. Jukić, T. van Waterschoot, T. Gerkmann, and S. Doclo, "Multi-channel linear prediction-based speech dereverberation with sparse priors," *IEEE/ACM Transactions on Audio, Speech and Language Processing*, vol. 23, no. 9, pp. 1509–1520, 2015.
- [11] J. Heymann, L. Drude, and R. Haeb-Umbach, "Neural network based spectral mask estimation for acoustic beamforming," in *Proc. IEEE ICASSP*, 2016, pp. 196–200.
- [12] K. Kinoshita, M. Delcroix, H. Kwon, T. Mori, and T. Nakatani, "Neural network-based spectrum estimation for online wpe dereverberation," in *Proc. Interspeech*, 2017, pp. 384–388.
- [13] K. Žmolíková, M. Delcroix, K. Kinoshita, T. Ochiai, T. Nakatani, L. Burget, and J. Černocký, "SpeakerBeam: Speaker aware neural network for target speaker extraction in speech mixtures," *IEEE Journal of Selected Topics in Signal Processing*, vol. 13, no. 4, pp. 800–814, 2019.
- [14] T. Yoshioka, H. Erdogan, Z. Chen, X. Xiao, , and F. Alleva, "Recognizing overlapped speech in meetings: A multichannel separation approach using neural networks," in *Proc. Interspeech*, 2018.
- [15] Y. Xu, J. Du, L.-R. Dai, and C.-H. Lee, "A regression approach to speech enhancement based on deep neural networks," *IEEE/ACM Transactions on Audio, Speech, and Language Processing*, vol. 23, no. 1, 2015.
- [16] J. R. Hershey, Z. Chen, J. L. Roux, and S. Watanabe, "Deep clustering: Discriminative embeddings for segmentation and separation," in *Proc. IEEE ICASSP*, 2016, pp. 31–35.
- [17] M. Kolbæk, D. Yu, Z.-H. Tan, and J. Jensen, "Multitalker speech separation with utterance-level permutation invariant training of deep recurrent neural networks," *IEEE Trans. Audio, Speech, and Language Processing*, pp. 1901–1913, 2017.
- [18] K. Kinoshita, M. Delcroix, S. Gannot, E. A. P. Habets, R. Haeb-Umbach, W. Kellermann, V. Leutnant, R. Maas, T. Nakatani, B. Raj, A. Sehr, and T. Yoshioka, "A summary of the REVERB challenge: State-of-the-art and remaining challenges in reverberant speech processing research," *EURASIP Journal on Advances in Signal Processing*, 2016.
- [19] J. Barker, R. Marxer, E. Vincent, and S. Watanabe, "The third 'CHiME' speech separation and recognition challenge: Dataset, task and baselines," in *Proc. IEEE ASRU-2015*, 2015, pp. 504–511.
- [20] N. Kanda, C. Boeddeker, J. Heitkaemper, Y. Fujita, S. Horiguchi, K. Nagamatsu, and R. Haeb-Umbach, "Guided source separation meets a strong asr backend: Hitachi/Paderborn university joint investigation for dinner party ASR," in *Proc. Interspeech*, 2019.
- [21] R. Haeb-Umbach, S. Watanabe, T. Nakatani, M. Bacchiani, B. Hoffmeister, M. Seltzer, H. Zen, and M. Souden, "Speech processing for digital home assistants," *IEEE Signal Processing Magazine*, 2019.
- [22] M. Togami, "Multichannel online speech dereverberation under noisy environments," in *Proc. EUSIPCO*, 2015, pp. 1078–1082.

- [23] S. Braun and E. A. P. Habets, "Linear prediction based online dereverberation and noise reduction using alternating Kalman filters," *IEEE/ACM Transactions on Audio, Speech, and Language Processing*, vol. 26, no. 6, pp. 1119–1129, 2018.
- [24] T. Dietzen, S. Doclo, M. Moonen, and T. van Waterschoot, "Joint multi-microphone speech dereverberation and noise reduction using integrated sidelobe cancellation and linear prediction," in *Proc. IWAENC*, 2018.
- [25] T. Yoshioka, T. Nakatani, M. Miyoshi, and H. G. Okuno, "Blind separation and dereverberation of speech mixtures by joint optimization," *IEEE Trans. on Audio, Speech, and Language Processing*, vol. 19, no. 1, January 2011.
- [26] N. Ito, S. Araki, T. Yoshioka, and T. Nakatani, "Relaxed disjointness based clustering for joint blind source separation and dereverberation," in *Proc. IWAENC*, 2014.
- [27] H. Kagami, H. Kameoka, and M. Yukawa, "Joint separation and dereverberation of reverberant mixtures with determined multichannel non-negative matrix factorization," in *Proc. IEEE ICASSP*, 2018, pp. 31–35.
- [28] T. Nakatani, R. Ikeshita, K. Kinoshita, H. Sawada, and S. Araki, "Computationally efficient and versatile framework for joint optimization of blind speech separation and dereverberation," in *Submitted to Interspeech*, 2020.
- [29] Z. Koldovsky and P. Tichavský, "Gradient algorithms for complex non-Gaussian independent component/vector extraction, question of convergence," *IEEE Trans. on Signal Processing*, vol. 67, no. 4, pp. 1050–1064, 2019.
- [30] T. Nakatani and K. Kinoshita, "Maximum likelihood convolutional beamformer for simultaneous denoising and dereverberation," in *Proc. EUSIPCO*, 2019.
- [31] C. Boeddeker, T. Nakatani, K. Kinoshita, and R. Haeb-Umbach, "Jointly optimal dereverberation and beamforming," in *Proc. ICASSP*, 2020. [Online]. Available: <https://arxiv.org/abs/1908.02710>
- [32] T. Nakatani, R. Takahashi, T. Ochiai, K. Kinoshita, R. Ikeshita, M. Declroix, and S. Araki, "DNN-supported mask-based convolutional beamforming for simultaneous denoising, dereverberation, and source separation," in *Proc. IEEE ICASSP*, 2020.
- [33] J. S. Bradley, H. Sato, and M. Picard, "On the importance of early reflections for speech in rooms," *The Journal of the Acoustic Society of America*, vol. 113, pp. 3233–3244, 2003.
- [34] T. Nishiura, Y. Hirano, Y. Denda, and M. Nakayama, "Investigations into early and late reflections on distant-talking speech recognition toward suitable reverberation criteria," in *Proc. Interspeech*, 2007, pp. 1082–1085.
- [35] Y. Avargel and I. Cohen, "On multiplicative transfer function approximation in the short-time fourier transform domain," *IEEE Signal Processing Letters*, vol. 14, pp. 337–340, 2007.
- [36] I. Cohen, "Relative transfer function identification using speech signals," *IEEE Trans. on Speech, and Audio Processing*, vol. 12, no. 5, pp. 451–459, 2004.
- [37] T. Nakatani, T. Yoshioka, K. Kinoshita, M. Miyoshi, and B. H. Juang, "Blind speech dereverberation with multi-channel linear prediction based on short time Fourier transform representation," in *Proc. IEEE ICASSP*, 2008, pp. 85–88.
- [38] T. Hori, S. Araki, T. Yoshioka, M. Fujimoto, S. Watanabe, T. Oba, A. Ogawa, K. Otsuka, D. Mikami, K. Kinoshita, T. Nakatani, A. Nakamura, and J. Yamato, "Low-latency real-time meeting recognition and understanding using distant microphones and omni-directional camera," *IEEE Trans. on Audio, Speech, and Language Processing*, vol. 20, no. 2, pp. 499–513, 2011.
- [39] T. Nakatani and K. Kinoshita, "A unified convolutional beamformer for simultaneous denoising and dereverberation," *IEEE Signal Processing Letters*, vol. 26, no. 6, pp. 903–907, April 2019.
- [40] B. J. Cho, J. Lee, and H. Park, "A beamforming algorithm based on maximum likelihood of a complex Gaussian distribution with time-varying variances for robust speech recognition," *IEEE Signal Processing Letters*, vol. 26, no. 9, pp. 1398–1402, August 2019.
- [41] F. Bahmaninezhad, J. Wu, R. Gu, S.-X. Zhang, Y. Xu, M. Yu, and D. Yu, "A comprehensive study of speech separation: spectrogram vs waveform separation," in *Interspeech*, 2019.
- [42] Y. Luo and N. Mesgarani, "Conv-TasNet: Surpassing ideal time-frequency magnitude masking for speech separation," *IEEE/ACM Trans. on Audio, Speech, and Language Processing*, vol. 27, no. 8, pp. 1256–1266, 2019.
- [43] T. Robinson, J. Fransen, D. Pye, J. Foote, and S. Renals, "WSJCAMO: A British English speech corpus for large vocabulary continuous speech recognition," in *IEEE ICASSP*, 1995, pp. 81–84.
- [44] N. Ito, S. Araki, M. Delcroix, and T. Nakatani, "Probabilistic spatial dictionary based online adaptive beamforming for meeting recognition in noisy and reverberant environments," in *Proc. IEEE ICASSP*, 2017, pp. 681–685.
- [45] S. Markovich-Golan and S. Gannot, "Performance analysis of the covariance subtraction method for relative transfer function estimation and comparison to the covariance whitening method," in *Proc. IEEE ICASSP*, 2015, pp. 544–548.
- [46] Y. Hu and P. C. Loizou, "Evaluation of objective quality measures for speech enhancement," *IEEE Tran. Audio, Speech, and Language Processing*, vol. 16, no. 1, pp. 229–238, 2008.
- [47] D. Povey, A. Ghoshal, G. Boulianne, L. Burget, O. Glembek, N. Goel, M. Hannemann, P. Motlicek, Y. Qian, P. Schwarz, J. Silovsky, G. Stemmer, and K. Vesely, "The Kaldi speech recognition toolkit," in *Proc. IEEE ASRU*, 2011.